Assembly Properties of Fluorescein-labeled Tubulin In Vitro before and after Fluorescence Bleaching

ROGER J. LESLIE, WILLIAM M. SAXTON, TIMOTHY J. MITCHISON, BONNIE NEIGHBORS, EDWARD D. SALMON, and J. RICHARD McINTOSH
Department of Molecular, Cellular and Developmental Biology, University of Colorado, Boulder, Colorado 80309. Dr. Leslie's current address is Department of Biological Sciences, University of California, Santa Barbara 93106.

ABSTRACT Brain tubulin has been conjugated with dichlorotriazinyl-aminofluorescein (DTAF) to form a visualizable complex for the study of tubulin dynamics in living cells. By using several assays we confirm the finding of Keith et al. (Keith, C. H., J. R. Feramisco, and M. Shelanski, 1981, *J. Cell Biol.*, 88:234–240) that DTAF-tubulin polymerizes like control tubulin in vitro. The fluorescein moiety of the complex is readily bleached by the 488-nm line from an argon ion laser. When irradiations are performed over short times (<1 s) and in the presence of 2 mM glutathione, a mixture of DTAF-tubulin and control protein (as occurs after microinjection of the fluorescent conjugate into living cells) will retain full polymerization activity. Slow bleaching (~5 min) or bleaching without glutathione promotes formation of covalent cross-links between neighboring polypeptides and kills the polymerization activity of DTAF-tubulin, including some molecules that are neither cross-linked nor bleached. Even under conditions that damage DTAF-tubulin, however, DTAF-microtubules are not destroyed by bleaching. They will continue to elongate by addition of DTAF-tubulin subunits to their free ends, and they neither bind nor exchange subunits along their lateral surfaces. These results suggest that DTAF-tubulin is a suitable analog for tubulin, both in studies of protein incorporation and for investigations of fluorescence redistribution after photobleaching.

Assembly of microtubules has been extensively studied in vitro. Polymerization proceeds by addition of tubulin as either dimer or oligomer to one or both ends of an existing microtubule (1, 3, 5, 45, 58). Efficient initiation of microtubule growth is more complex, usually requiring either proteins in addition to tubulin (34, 44, 56) or a seeding structure to nucleate polymerization (reviewed in reference 31). Microtubule assembly in vivo has received comparatively little attention. The polymerization reactions identified in vitro are widely believed to pertain in cells, but only general properties of microtubules are well established in vivo, e.g., lability to cold (14), colchicine (13), high hydrostatic pressure (37), and elevated concentrations of Ca^{++} (16, 22). Initiation of polymerization for cytoplasmic and mitotic microtubules is usually accomplished by specific structures such as the centrosome. Such organizing centers define the structural pattern of microtubule growth (reviewed in reference 31). The extent of microtubule assembly is clearly under cytoplasmic regulation, waxing and waning at specific times in the life of a cell or organism, but the pathways of subunit addition or loss and the mechanisms for assembly regulation are still matters of speculation.

The principal difficulty of studying microtubule assembly in vivo is finding a way to watch the process in living cells. Polarization optics has provided a high time-resolution view of the behavior of spindle microtubules, both as they form and disassemble in normal mitotic cycles (41), and as they respond to experimental perturbations of their assembly (13, 16, 22, 37). These studies have shown that spindle dynamics are fast: a spindle can be induced to disassemble and reassemble within 1 min, entering normal anaphase shortly thereafter (16, 22). Such work has led to an in vivo model of a dynamic equilibrium between assembled and disassembled states of microtubule subunits (15). The pathways of spindle microtubule formation and disassembly, however have not yet been identified. Cytoplasmic microtubules are even more difficult to study, because the signal produced by the birefringence or phase retardation of one or a few microtubules is usually too

THE JOURNAL OF CELL BIOLOGY · VOLUME 99 DECEMBER 1984 2146-2156

weak to detect against the background of the cytoplasm.

To overcome the difficulties of studying microtubules in vivo, one wants a method that renders specific components of the cytoskeleton readily visible in living cells. A useful strategy is fluorescent analog cytochemistry where fluorescently labeled proteins are incorporated into living cells to function as tracers of corresponding endogenous proteins and the distribution of labeled protein is measured using fluorescence microscopy (21, 26, 46, 47, 51, 53, 54, 59). Fluorescence redistribution after photobleaching offers an additional technique for exploiting fluorescent proteins to study polymer behavior in vivo (19, 27, 52, 61 reviewed in references 20 and 55). For our work on tubulin polymerization, we have selected the fluorochrome dichlorotriazinyl-aminofluorescein (DTAF)[1] because of the clear indications from published work that DTAF-tubulin behaves normally both in vitro and in vivo (21, 51). In addition, the wavelength for excitation of fluorescein is less damaging to cells than the shorter wavelengths necessary for some of the other fluorochromes that have been used to label tubulin (49, 50). Further, work using fluorescence redistribution after photobleaching to study the dynamics of tubulin in vivo can be achieved with comparatively little light for bleaching, because fluorescein in an aqueous environment at neutral pH bleaches so easily.

In this paper we characterize DTAF-tubulin in vitro, comparing it with control protein before and after photobleaching by laser light. We confirm the studies of Keith et al. (21), which showed that the behavior of labeled, unbleached protein is indistinguishable from that of control protein with the assays used. Laser photobleaching of DTAF-tubulin under experimental circumstances that approximate the conditions in a living cell causes little observable damage to the tubulin or its neighboring molecules, encouraging the view that this fluorescent conjugate is also suitable for bleaching studies in vivo. On the other hand, bleaching of fluorescent tubulin under other conditions inactivates the protein for polymerization and induces its covalent conjugation to nearby polypeptides. We define some of the parameters that must be controlled to minimize bleach-induced artifacts. In the following two articles we describe methods for quantitating the behavior of DTAF-tubulin in vivo. The diffusion coefficient for tubulin is measured in the cytoplasm of sea urchin eggs (38), and the rate of turnover of tubulin in spindles of the sea urchin zygote is shown to be surprisingly fast (39). In the final article, these methods are applied to mammalian cells in culture (40). Here we compare the dynamics of tubulin in mitotic and interphase cells and show that there are major changes in the kinetics of tubulin turnover as a function of stage in the cell cycle.

MATERIALS AND METHODS

Preparation of Fluorescent Tubulin: Tubulin and its associated proteins were purified from bovin brain by two cycles of temperature-dependent assembly and disassembly as described by Weingarten et al. (57). Fluorescent tubulin was prepared from this microtubule protein much as described by Keith et al. (21). Assembled microtubules (MTs) were labeled with DTAF by mixing the fluorochrome at 10 mg/ml in dimethylsulfoxide with MTs in 0.1 M 2-(*N*-morpholino)ethanesulfonate, 1 mM EGTA, 1 mM $MgSO_4$, and 0.1 mM GTP at pH 6.9, containing 4 M glycerol. The molar ratio of DTAF to tubulin was 50:1. The reaction mixture was adjusted to pH 7.0 and then incubated at 37°C for 10 min. A pellet containing labeled MTs was collected by centrifugation at 125,000 *g* for 30 min at 37°C in a Beckman 50.2 Ti rotor (Beckman Instruments, Inc., Fullerton, CA). Active DTAF-tubulin was then purified away from inactive tubulin and contaminating proteins by four assembly–disassembly cycles in 1 M glutamate, 0.1 mM GTP, and 1 mM EGTA following the method of Hamel and Lin (11). Dye-to-protein ratios for the final product were estimated by measuring protein concentration with the method of Bradford (4) and dye concentration with a spectrophotometer, using a molar extinction coefficient for DTAF of 27,000, as measured by us for pure DTAF in 0.1 M PIPES, 1 mM EGTA, 1 mM $MgSO_4$, and 0.1 mM GTP at pH 6.9 (PME-GTP). Control protein was collected and purified as described for DTAF-tubulin, but the labeling step was omitted.

Microtubule Assembly Promoters and Initiators: Heat-stable microtubule-associated proteins (MAPs) were prepared as described by Kim et al. (24) with the modification that after centrifugation to remove the heat denatured proteins, MAPs were harvested by precipitation with 50% saturated $(NH_4)_2SO_4$, dialyzed against PME-GTP, and stored at −70°C.

Flagellar axonemes were prepared from sperm of the sea urchin *Lytechinus variegatus* by the method of Gibbons (9). Centrosomes were isolated from cultured neuroblastoma cells, strain N115, by a method described in detail elsewhere (33). Briefly, 5×10^8 Chinese hamster ovary cells grown on dishes were rinsed in PBS at 4°C followed by hypotonic lysis in 1 mM Tris-HCl, pH 8.0, containing 0.1% β-mercaptoethanol. PIPES buffer at pH 7.2 was then added to 10 mM and EDTA to 1 mM. Nuclei and debris were pelleted from the lysate at 1,000 *g* for 3 min, then the supernatant was layered over the same buffer containing 20% (wt/wt) Ficol and spun at 23,500 *g* for 15 min in a Sorval HB4 rotor (DuPont Instruments, Sorvall Biomedical Div., Newtown, CT). The supernatant was discarded and the material at the top of the cushion was collected and layered on a 20–65% (wt/wt) sucrose gradient in the same buffer, then spun for 2 h at 90,000 *g* in a Beckman SW28 rotor. The centrosomes usually were in the 54–50% (wt/wt) samples.

Microtubule Assembly Assays: Just before an experiment, 20–100-μl aliquots of protein were thawed and dialyzed against 1,000 vol of PME-GTP for 30 min at 4°C. Assembly mixtures of DTAF- and control tubulin contained 2.0 mg/ml tubulin, 0.2 mg/ml MAPs, and 1 mM GTP. The mixtures were clarified in a Beckman microfuge at 11,000 *g* for 10 min at 4°C, and degassed under aspirator vacuum for 5 min. 300 μl of each sample was added to quartz microcuvettes at 0°C, and its optical density (OD) at 350 nm monitored at 36°C in the temperature-controlled chamber of a Gilford spectrophotometer (Gilford Instrument Laboratories, Inc. Oberlin, OH). For numerical comparison of different samples, assembly rates measured as OD/min were normalized by dividing the measured rate by the maximum OD_{350} achieved by each sample.

The assembly of DTAF-tubulin onto axonemes was studied by diluting purified axonemes in PME-GTP into 0.5 mg/ml DTAF-tubulin and 5 μg/ml MAPs in PME with 1 mM GTP. This mixture was incubated at 30°C for 20 min, then a 5-μl sample was placed on a 22 × 22-mm glass coverslip and the axonemes were allowed several seconds to adsorb to the glass. Assembly was stopped by rinsing the coverslip with a solution of tubulin-free PME containing 20 μM taxol and 4 mM L-ascorbate. These preparations were examined on a Zeiss Universal microscope (Carl Zeiss, Inc., New York) equipped with epifluorescence and dark-field optics. To view the fluorescein we used the Zeiss fluorescein isothiocyanate (FITC) filter pack and a × 100 plan objective with a back focal plane iris opened wide (NA = 1.25). For dark-field optics, we used transillumination through a Zeiss ultracondenser (Carl Zeiss, Inc.) and the same objective with the iris stopped down all the way (NA = 0.6). Illumination for dark-field and fluorescence microscopy was provided by an Osram (Berlin, W.G.) HBO-200 mercury arc lamp. To record images with a minimum of fluorescence bleaching, we used a Venus DV-2 intensified television camera (Farmingdale, NY). The video signal was displayed on two monitors, one for viewing and a Conrac SNA 9/C for photography (Corvinia, CA). The gain in signal strength provided by the TV camera made it possible to take a 35-mm negative of very dim objects in about 0.03 s, but the increase in image noise accompanying the gain made such images poor in quality. We compromised between image quality and specimen bleaching by taking 0.5-s photographs of the Conrac TV monitor with a Nikon 35-mm camera (Nikon Inc., Garden City, NY), using Kodak Plus-X film (Eastman Kodak Co., Rochester, NY) developed in HC 110 dilution B. These images summed the signals from 15 successive video frames, improving the signal-to-noise ratio by a factor of about 4.

We studied the polymerization of tubulin on centrosomes by mixing centrosomes first with DTAF-tubulin and then with unlabeled protein, or first with unlabeled and then with fluorescent protein. Both preparations of tubulin were in 80 mM PIPES, 1 mM EGTA, 1 mM $MgCl_2$, and 1 mM GTP, and no MAPs were added. A sample of tubulin was mixed with ⅓ vol of centrosomes to produce a final tubulin concentration of 2 mg/ml. After 10 min at 37°C, DTAF-tubulin at 1.5 mg/ml was added in sufficient volume that the final DTAF-

[1] *Abbreviations used in this paper*: DTAF, dichlorotriazinyl-aminofluorescein; FITC, fluorescein isothiocyanate; MAP, microtubule-associated protein; MT, microtubule; PME, buffer containing PIPES, $MgSO_4$, and EGTA.

tubulin concentration was four times the concentration of unlabeled material. In the reciprocal experiments, the orders of tubulin addition were simply reversed. Samples were fixed in ethylene glycol-*bis* succinamidyl succinate at a final concentration of 2 mg/ml and centrifuged through a glycerol cushion onto a polylysine-coated coverslip. Some coverslips were stained for immunofluorescence with a monoclonal anti-α-tubulin and a rhodamine-labeled goat anti-mouse (Miles Laboratories Inc., Elkhart, IN), then mounted in 90% glycerol, 0.1 M $NaHCO_3$, and 2% *n*-propyl gallate (10).

Growth of MTs from isolated centrosomes was followed directly by mixing a preparation of active centrosomes, prepared as described above, with DTAF-tubulin at 1 mg/ml in PME-GTP and putting 5 μl of the mixture on a 22 × 22-mm glass coverslip treated with Sigmacoat (Sigma Chemical Co., St. Louis, MO). The coverslip was inverted onto a slide also treated with Sigmacoat, and the liquid was allowed to spread as a thin layer between the two surfaces of coated glass. The coverslip was then sealed down with a mixture of petroleum jelly, lanolin, and parafin 1:1:1. The resulting liquid layer was ~5 μM thick as measured with the fine-focus micrometer of the Zeiss microscope. Some centrosomes adsorbed to the under surface of the coverslip and were thus in an optimum position for high-resolution microscopy. Polymerization on these was followed with epifluorescence optics using the Zeiss × 63 plan apochromat objective (NA = 1.4).

Laser Microbeam Irradiation: For photobleaching of microscopic samples, the 488-nm line of a 2-W argon ion laser (Spectra-Physics Inc., Mountain View, CA, model 164) was reflected from mirrors so as to become co-axial with the epi-illumination path of the fluorescence microscope, as described in detail by Salmon et al. (38). When a × 63 lens was used, the waist of the beam at the specimen plane was ~10 μm in diameter. The convergence of the laser beam was very gradual because of the long focal length of the beam-controlling optics, resulting in a beam geometry that was essentially cylindrical at the plane of the specimen (40). Times and powers of irradiation were determined by trial and error.

Laser Photobleaching of Fluorescence in Solution: Photobleaching of DTAF fluorescence in solution was achieved with the 2-W laser operating at full power (~650 mW in the 488-nm line). For some experiments, the 1-mm diam beam from the laser was spread by a 1-in Spectra-Physics beam-expanding telescope adjusted to produce a collimated beam as wide as the sample. Because the total beam energy was spread over a big area, bleaching times in this configuration were several minutes. In other experiments, the solution of fluorescent protein was flowed through a drawn capillary whose inner diameter approximated the diameter of the laser microbeam described in Salmon et al. (38). The high light intensity of the microbeam acting on the capillary allowed all the protein that passed the beam to be bleached to ~50% fluorescence during 0.5-s of irradiation, a typical time of exposure used in photobleaching cells.

Relation between Fluorescence and Absorbance for DTAF: A known weight of DTAF measured on a Mettler H34 balance (Mettler Instrument Corp., Highstown, NJ) was solubilized in PME and serial dilutions were made. The OD_{490} of each dilution was measured in a Gilford model 222 spectrophotometer and the relative fluorescence at 514 nm determined in a Perkin-Elmer MPF-43A fluorescence spectrophotometer (Perkin-Elmer Corp., Norwalk, CT) with excitation at 490 nm ± 4 nm. 1-ml samples of 10.5 μM DTAF in PME were bleached in the full beam of the laser for times varying from 0 to 80 min. The relative fluorescence versus OD_{490} roughly paralleled the standard curves (see below).

Electron Microscopy: Axonemes and MTs were prepared for electron microscopy and negatively stained with uranyl acetate as described by Allen and Borisy (1). In some experiments MTs adsorbed to finder grids were bleached for 0.5 s in the full-intensity laser microbeam before negative staining.

MT Length Distribution: MTs were assembled from 0.2 mg/ml DTAF-tubulin and 2.25 mg/ml cycle 2 tubulin in PME-GTP. After 15 min at 37°C, the MTs were sheared by four passes through a 23.5-gauge needle. Equal volumes of the assembly mixture were placed in two cuvettes and allowed to incubate for another 5 min. One sample was bleached for 5 min in the spread beam of the argon laser operating at full power. 10-μl aliquots were taken from the control and bleached samples and negatively stained for electron microscopy (1). Micrographs were taken at × 2,000 with a JEM 100C electron microscope (JEOL, Peabody, MA). These negatives were projected at × 8,000 and MT lengths were measured with a micrometer. The mean and standard deviation of 100 MT lengths from each sample were determined. The significance of the difference between the means was evaluated using the likelihood ratio technique (8).

Electrophoresis and Immune Blotting: Proteins were separated by electrophoresis on slab gels containing SDS and an acrylamide gradient from 4 to 11% (SDS PAGE) essentially as described by Laemmli (28). The resolved fluorescent proteins were visualized with a ultraviolet light box and photographed with Polaroid positive-negative film (Polaroid Corp., Cambridge, MA). The gels were then fixed and stained with Coomassie Brilliant Blue and photographed again with visible light. Relative molecular weights were estimated by protein mobility as compared with several standards: egg albumin, phosphorylase B, tubulin, BSA, and myosin (42). For antibody staining, protein bands in the SDS PAGE slabs were electrophoretically transferred to nitrocellulose paper by the method of Towbin et al. (48), as modified by Erickson et al. (7) and Batteiger et al. (2). The nitrocellulose sheets were treated with mouse antibodies against specific MT proteins and secondarily stained with ^{125}I-goat anti-mouse IgG as previously described (18). Autoradiograms were prepared on Kodak Noscreen x-ray film; then the nitrocellulose sheet was stained with fast green. Two-dimensional separations of proteins were run according to the method of O'Farrell (35).

RESULTS

Characterization of DTAF-Tubulin

Aliquots of DTAF-labeled MTs and unlabeled control protein were taken after each successive cold–warm cycle during the tubulin purification after labeling. When these samples were compared by electrophoresis on 4–11% acrylamide gradient SDS PAGE, the fraction of Coomassie stain in the tubulin bands increased from ~60% to between 95 and 98%. The fraction of fluorescence in the tubulin bands increased from ~20% to between 80 and 90% of the total protein-bound fluorescence (Fig. 1). The molar ratio of DTAF to tubulin varied between 1.0 and 1.8 in different preparations. The principal contaminant in the cycle 4 material was a band of ~145,000 mol wt, which is clearly visible in the fluorescence pictures (Fig. 1 *a*) but faint in Coomassie stain (Fig. 1 *b*). This band binds anti-tubulin in immunoblots (see below) and may be an oligomer of tubulin.

Electron microscopy of negatively stained DTAF-tubulin in conditions promoting assembly revealed MTs that were morphologically indistinguishable from those assembled with control tubulin (Fig. 1, *c* and *d*). Electrophoresis of the

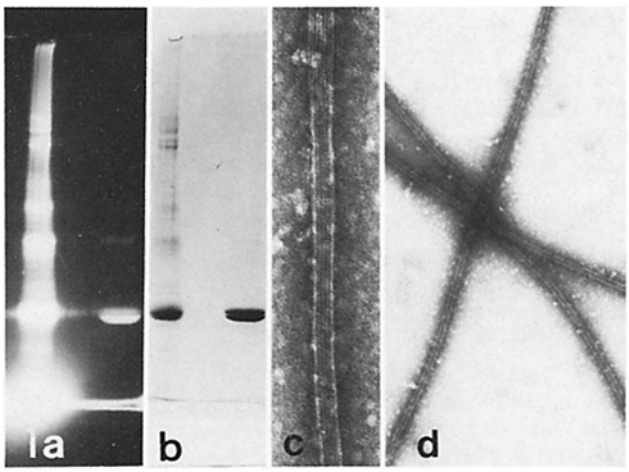

FIGURE 1 Purification of DTAF-tubulin. (*a*) Fluorescence photograph of DTAF-tubulin on a 4–11% SDS gel. The first lane contains a sample of twice-cycled bovine brain tubulin taken immediately after the DTAF-labeling step. The second lane contains a sample of cycle 4, glutamate-purified DTAF-tubulin. 88% of the fluorescence associated with protein in the second lane is in the tubulin bands, and most of the remaining fluorescence runs at 145,000 mol wt. The β monomer of tubulin is more fluorescent than the α monomer. (*b*) Coomassie stain of the gel from *a*. 97% of the Coomassie stain in lane *2* is contained in the tubulin bands; most of the rest runs at 145,000 mol wt. (*c*) An electron micrograph of assembled, negatively stained DTAF-tubulin. Protofilaments like those observed in similar preparations of normal MTs are present here. × 100,000. (*d*) A lower-magnification electron micrograph of several MTs assembled from DTAF-tubulin and negatively stained. × 30,000.

purified DTAF-tubulin on two-dimensional gels shows that both α- and β-subunits of tubulin are labeled, though β is often more heavily labeled than α (Fig. 2). Although the Coomassie stain and the fluorescence overlap, the fluorescent spots are shifted slightly to the right of the unlabeled material on the gel, suggesting that DTAF causes the acidification expected from a reaction with protein amine groups. The flare on the right edge of the β-tubulin spot may be the result of overlabeling of a small amount of the protein.

The assembly–disassembly characteristics of DTAF-tubulin and control protein were followed in a spectrophotometer by measurements of turbidity at 350 nm (Fig. 3). After a lag, the initial rates of assembly, normalized as described in Materials and Methods, were 0.15 ± 0.02 OD units/min for both labeled and control tubulin; the normalized rates were consistently indistinguishable. Without normalization, either DTAF-tubulin or control protein would be slightly faster, but there was no preference of one protein over the other. The ability of DTAF-tubulin to behave in a manner indistinguishable from unmodified tubulin during microtubule polymerization was verified using an in vitro treadmilling assay (30, 60). Briefly, bovine brain microtubule protein was assembled to steady state in vitro in the presence of 10% DTAF-tubulin, or 10% control tubulin. The DTAF-tubulin co-polymerized with microtubule protein as described by Keith et al. (21). At steady state, the flux rate of control microtubules was 0.69/s, and for DTAF-containing microtubules, 0.54/s, as determined by measuring the rate of [^{3}H]GTP incorporation into the microtubules (Miller, H. P., R. J. Leslie, and L. Wilson, unpublished data). DTAF-tubulin will not assemble into MTs without added MAPs unless centrosomal or axonemal seeds are present (see below).

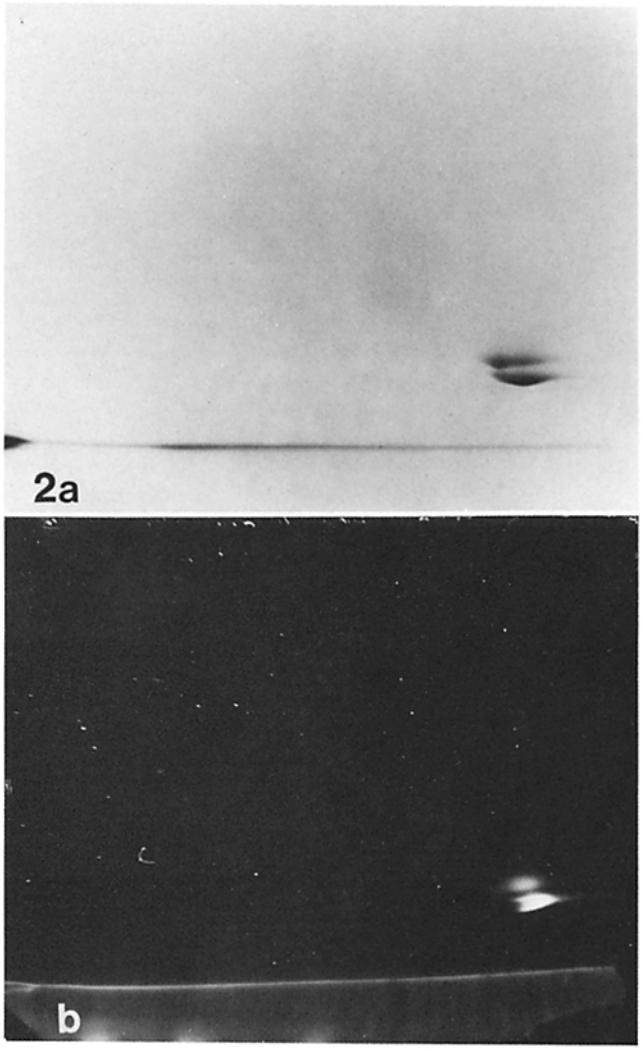

FIGURE 2 Two-dimensional gel electrophoresis. 20 μg of glutamate-purified DTAF-tubulin was applied to an isoelectric focusing gel containing one part of pH 3.5–10 ampholines and four parts of pH 5–7 ampholines. The second dimension was an SDS, 4–10% acrylamide gradient gel. (*a*) The gel stained with Coomassie Brilliant Blue displays two broad spots corresponding to α- and β-tubulin monomers. (*b*) A fluorescence image of the gel in a demonstrates that both monomers are labeled with DTAF. A small amount of fluorescence can be seen in the upper right quadrant of the gel, probably corresponding to the 145,000-mol-wt band observed on one-dimensional SDS gels. The fluorescently labeled monomers are more acid than the unlabeled proteins observed in *a*.

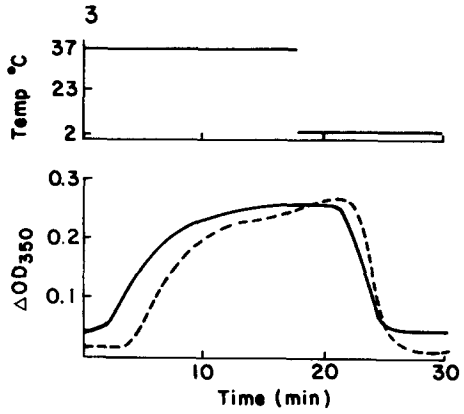

FIGURE 3 Assembly–disassembly of DTAF-tubulin and control tubulin. DTAF-tubulin and control tubulin were dialyzed into PME-GTP buffer and diluted to 2 mg/ml. Heat-stable MAPs were added to 0.2 mg/ml. Turbidity of these solutions at 350 nm was followed in the temperature-controlled chamber of the spectrophotometer. The upper graph displays the temperature of circulating water over the time period of the lower graph. DTAF-tubulin (solid line) assembles sooner than the control (dashed line) but the rates of assembly and disassembly are quite similar.

DTAF-tubulin elongates sea urchin flagellar axonemes in vitro, producing fluorescent tufts at each end of the axonemal seed (Fig. 4, *a* and *b*). Electron microscopy confirmed that these tufts contain MTs (Fig. 4*c*). The distribution of fluorescence in Fig. 4*b* demonstrates that existing MTs bind DTAF-tubulin only at their ends, not along their walls. It also confirms that DTAF tubulin resembles control tubulin in elongating existing MTs in vitro with "biased polar growth" (1, 3, 45), i.e., it adds faster to one end of the axoneme than to the other.

Centrosomes prepared as described were sufficiently active sites of MT initiation that we were able to study the zone of addition for DTAF-tubulin in vitro to both centrosomes and existing asters of MTs. Fig. 5*a* shows the rhodamine fluorescence image of an aster assembled first with DTAF-tubulin, then with unlabeled tubulin, and then stained with antitubulin using rhodamine-labeled secondary antibody. Fig. 5*b* is the fluorescein image of the same aster, showing a concentration of DTAF-tubulin in the centrosome-proximal region. Fig. 5*c* is the fluorescein image of another aster made by adding the DTAF-tubulin after unlabeled tubulin. We conclude that tubulin adds to centrosomal MTs in vitro at the ends distal to the centrosome. These pictures suggest that DTAF-tubulin behaves like unlabeled tubulin for polymerization in vitro,

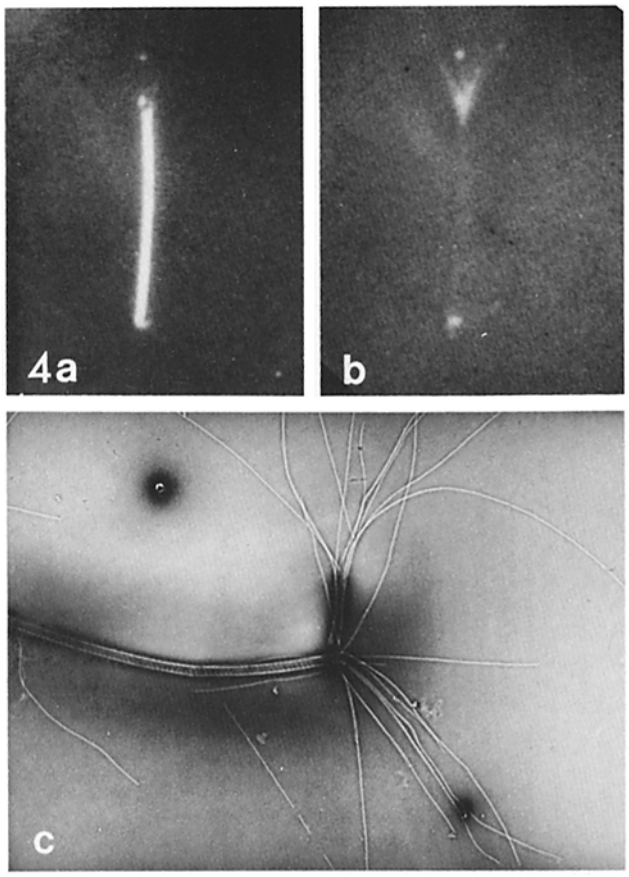

FIGURE 4 MT growth from the ends of an axoneme. (*a*) A dark-field image of an isolated sea urchin axoneme that has been incubated in DTAF-tubulin (0.5 mg/ml) and MAPs (5 μg/ml) followed by a wash in PME buffer containing taxol and ascorbate. The low-resolution television system does not image the tufts of MTs that extend from each end of the axoneme. (*b*) A fluorescence image of the axoneme in *a*. Fluorescent tufts are visible extending from each end of the axoneme and a small amount of fluorescence appears in the axoneme. (*c*) An electron micrograph of two axoneme fragments that have been negatively stained with uranyl acetate. MTs of normal morphology extend from one end of each axoneme. The axonemes were "dodged" during photographic printing to permit visualization of some of their structural detail in a print that also shows the microtubules. × 1,100. (*a* and *b*). × 6,000.

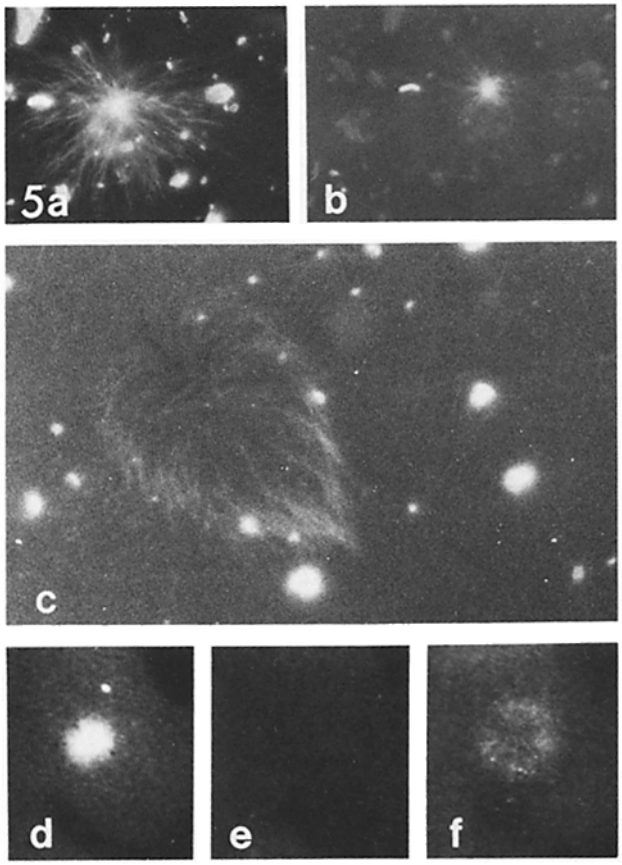

FIGURE 5 Assembly of DTAF-tubulin on isolated centrosomes. Centrosomes were first incubated for 10 min at 37°C in an assembly mixture containing 2 mg/ml DTAF-tubulin. The DTAF-tubulin was then diluted fourfold with unlabeled tubulin and incubation was allowed to continue. The centrosomes were fixed and labeled with monoclonal anti-α-tubulin and rhodamine goat anti-mouse. Plate *a* is an image of aster fluorescence viewed with the rhodamine filter pack. Plate *b* is the same aster viewed with the FITC filter pack. Plate c is the reciprocal experiment in which MTs were assembled onto a centrosome first from unlabeled tubulin and then from DTAF-tubulin (FITC filter set). Both labeled and unlabeled tubulin add to the distal ends of MTs. The DTAF-tubulin does not appear to bind adventitiously to the walls of existing MTs. Asters growing in DTAF-tubulin and viewed with the FITC filter pack (*d*) were completely bleached (*e*) and allowed to continue assembling. In *f* a halo of fluorescence has formed around the bleached aster. We conclude that bleaching DTAF-MTs does not destroy them, does not block their elongation, and does not induce DTAF-tubulin in solution to attach to the surface of the bleached MTs. × 900.

because the protein added second assembles on the distal microtubule end, whether it is labeled or unlabeled tubulin.

Effects of Photobleaching on MT Polymerization In Vitro

We used the laser microbeam and a low-light level video system to study the effect of MT photobleaching on subsequent MT elongation. Assembly of DTAF-tubulin on centrosomes produces fluorescent asters that are bright enough to be visible against the background of the 5-μm thickness of DTAF-tubulin at 1 mg/ml (Fig. 5*d*). When such an aster is bleached early during its growth period using a 0.5-s irradiation with the 488 line of the Argon ion laser operating at half power, the fluorescence of the aster, the centrosome, and the background are obliterated (Fig. 5*e*). Background fluorescence returns by diffusion within seconds, but the fluorescence of the aster recovers slowly. The centrosome itself becomes brighter than background over several minutes, suggesting an exchange of bound, bleached tubulin for free, unbleached subunits. The bleached MTs remain bleached for hours, but they elongate within minutes, adding unbleached subunits to make a fluorescent anulus (Fig. 5*f*). We conclude that DTAF-MTs photobleached in PME-GTP in vitro do not recover their fluorescence. They are not destroyed by bleaching, and they retain their capacity to elongate. Subunit addition is again at the MT end distal to the centrosome.

We next evaluated the effect of photobleaching on the polymerization of the DTAF-tubulin dimer. Because polymerization was followed turbidimetrically by OD_{350}, it was convenient to monitor the extent of a bleach spectrophotometrically by reduction in OD_{490}, the absorption maximum of fluorescein. The relation for DTAF between OD_{490} and fluorescence, as measured in a spectrofluorimeter, is shown in Fig. 6. DTAF-tubulin and control tubulin were assembled

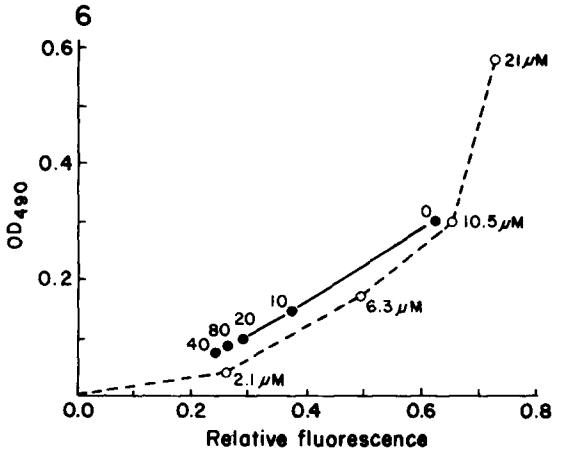

FIGURE 6 Relationship between OD_{490} and relative fluorescence of DTAF. DTAF was solubilized in PME to 21 μM and serial dilutions were made (solid line, ●). Aliquots of the 10.5-μM dilution were bleached in quartz cuvettes for 0–80 min in the full intensity beam of the 2-W argon laser (dashed line, ○). Both the bleaches and the dilutions are linear in the OD range normally encountered with DTAF-labeled tubulin. We conclude that OD_{490} is a good estimation of the relative fluorescence in the OD range 0.1–0.3.

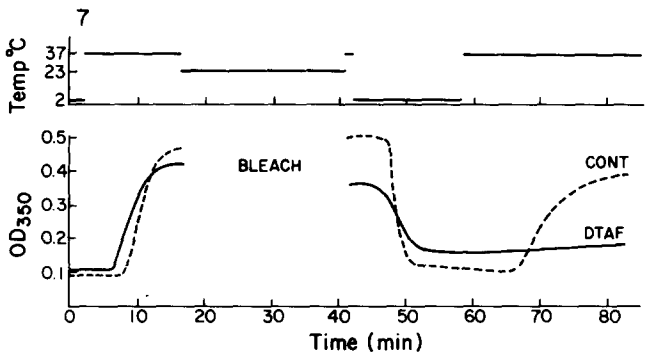

FIGURE 7 Assembly-disassembly of bleached DTAF-tubulin. The assembly assay was conducted as described in Fig. 3, but after assembly each solution was irradiated for 5 min in the full-intensity beam of the 2-W argon laser spread to a beam cross section of ~1 cm. The DTAF-tubulin was bleached to 80% of its original fluorescence (20% bleach). The DTAF-tubulin (solid line) disassembles slightly during irradiation whereas the control tubulin (CONT; dashed line) continues to assemble. Both control and DTAF-tubulin disassemble in the cold (2°C). The control tubulin reassembles at 37°C but the DTAF-tubulin reassembles only slightly after an irradiation.

in PME-GTP, then irradiated with the beam of the laser spread to 1 cm in diameter and operating a full power. 5–10 min of irradiation was required for each sample to bleach the DTAF-tubulin by 20%. Immediately after a bleach there was often a slight reduction in the OD_{350} of the DTAF-tubulin (Fig. 7). This is not due to fluorochrome bleaching (reduction in OD_{490}) because the OD_{350} of DTAF is not reduced by bleaching; it is actually slightly increased. We have not observed an induced polymerization artifact as described for 5-iodoacetamido fluorescein-labeled actin (29). Electron microscopy showed that both labeled and unlabeled samples contained microtubules of normal morphology in approximately equal numbers (data not shown). Both bleached and control MTs were labile when the temperature of the solutions was lowered to 2°C. When the temperature of the solutions was again raised to 37°C, however, the control tubulin reassembled, but the DTAF-tubulin did not (Fig. 7). Apparently prolonged irradiation of DTAF-tubulin in PME-GTP with bright 488-nm light destroys the capacity of the protein to polymerize.

Although the molecular mechanisms of photobleaching are not well understood, there are several indications that oxidations and free radical reactions may be at work (reviewed in reference 55). For reasons that are not clear, the rate at which a given amount of bleaching energy is delivered has an effect on the resulting chemistry (43), suggesting that our 5-min bleaches may be more deleterious than the short, intense bleaches achieved on cells with a laser microbeam. We have therefore tried the effect of sulfhydryl reagents, free radical scavengers, and short bleaches with intense light on the polymerization properties of DTAF-tubulin. By using the configuration for fast bleaching described in Materials and Methods we have reduced the duration of the bleach to 1 s or less, comparable with the bleaches used in vivo. The effects of reduced glutathione on MT polymerization are of particular interest, because current estimates of its concentration in vivo range from 0.5 to 10 mM, and the existence of glutathione reductase makes its effective concentration in vivo much higher (25, 32, 36).

Fig. 8*a* shows the effect of fast bleaching to ~80% fluorescence on DTAF-tubulin in PME-GTP, supplemented with 2 mM glutathione. As before, the DTAF-MTs retain their cold lability during the bleach, but under these conditions the bleached protein is still somewhat active in polymerization. Apparently short bleaches and glutathione reduce the damage done by the laser light. Further reduction is achieved by structuring an experiment more closely to simulate the conditions of an in vivo bleach. One usually injects a cell with a volume <10% that of the cell. If the injected protein concentration approximates that in vivo, only 1 tubulin dimer in about 10 will be labeled. Fig. 8*b* compares the results of mixing one part DTAF-tubulin with nine parts control tubulin to those results obtained with control protein alone. In these circumstances, the mixture of labeled and unlabeled protein retains full polymerization activity after bleaching.

Analysis of Factors Affecting the Action of Bleaching Light on the Behavior of DTAF-Tubulin

The differences between the polymerization behaviors shown in Figs. 7 and 8 show that the response of DTAF-tubulin to irradiation by 488-nm light is condition dependent. We have therefore varied bleaching conditions to assess the importance of several experimental factors. Fig. 9 shows a 4–11% gradient SDS PAGE of DTAF-MTs and control proteins, both before and after bleaching by ~20% in PME-GTP over 5 min with the spread laser beam. The Coomassie-stained lanes show that the laser has no effect on control protein. The DTAF-MT protein, however, is modified. Comparison of lanes *a* and *e* shows that irradiation intensifies the faint band at 145,000 mol wt, decreases the MAP2 band, and forms two high-molecular-weight bands as well as some material that will barely enter the gel. Comparison of lanes *c* and *g* shows a decrease in the fluorescence at 145,000 mol wt, in spite of the mass increase of that band, and there is an accumulation of fluorescent material at the top of the gel. These results suggest that laser bleaching is accompanied by the formation of covalent links between tubulin and other polypeptides.

The hypothesis of covalent cross-linking has been tested by

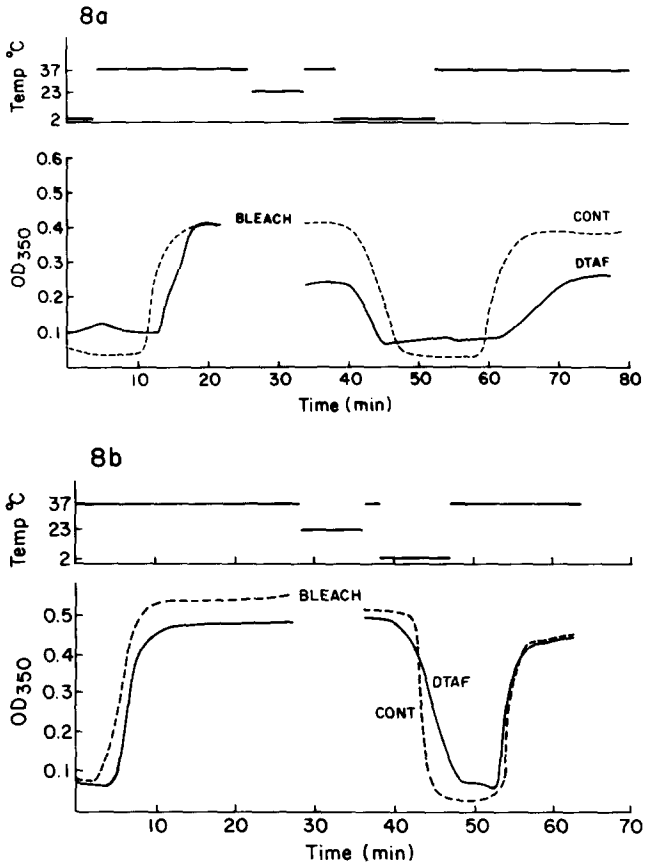

FIGURE 8 Assembly–disassembly of DTAF-tubulin fast-bleached in the presence of glutathione. DTAF-tubulin was mixed with either MAPs or control MT protein in PME supplemented with 1 mM GTP and 2 mM glutathione. Polymerization and its turbidometric recording were as in Fig. 7. (*a*) DTAF-tubulin at 2 mg/ml with 0.2 mg/ml heat-stable MAPs vs. 2.5 mg/ml cycle 3, MAP-containing MT protein. A 100-μl sample of each assembly mixture was irradiated for 0.5 s. Polymerizations and depolymerizations are comparable. The bleached DTAF-tubulin now retains ~58% of its initial activity. (*b*) DTAF-tubulin (0.2 mg/ml) and unlabeled, MAP-containing MT protein (2.25 mg/ml). Control protein is as described above. Irradiation of both samples was accomplished during ~0.5 s using the capillary flow cell and laser microbeam as described in Materials and Methods. Under these circumstances, labeled and control preparations are quite strictly comparable.

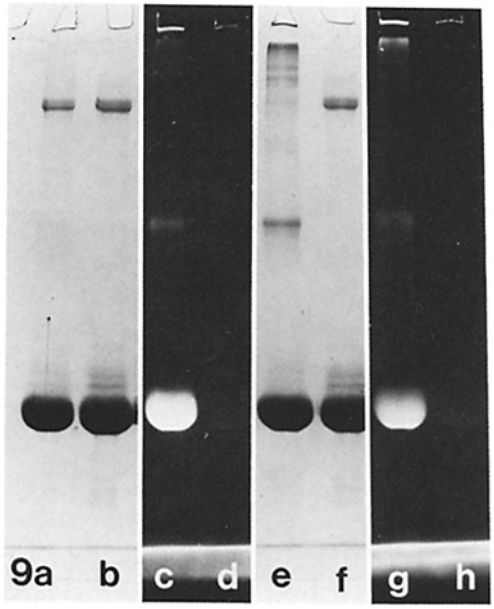

FIGURE 9 Gel electrophoresis of bleached DTAF-tubulin. MTs were assembled from purified DTAF-tubulin (2.0 mg/ml) and heat-stable MAPs (0.2 mg/ml) in PME-GTP (*a* and *c*) and from cycle 2 tubulin (*b* and *d*). These MTs were irradiated for 5 min in the full-intensity beam of the spread beam of a 2-W argon laser (*e–h*). The control protein is not altered by the irradiation (*f* and *h*). After irradiation, new bands are observed in Coomassie-stained gels at 145,000 and 330,000 mol wt, and at the top of the gel *g*.

immune blotting, as shown in Fig. 10. Control tubulin in PME-GTP was mixed with MAP2 and DTAF-tubulin at different ratios, polymerized, bleached by 20% over ~5 min with the spread laser beam, and then electrophoresed on a 4–11% acrylamide SDS gel. Immune blots of the separated proteins were prepared using a monoclonal anti-MAP2 (17), two different monoclonal anti-β-tubulins (an anti-*Drosophila* β-tubulin, the generous gift of Margaret Fuller, and an anti-sea urchin β-tubulin prepared in our lab [42]), and one anti-α-tubulin (anti-yeast α-tubulin, the generous gift of John Kilmartin, characterized as YL1/2 in reference 23). The anti-MAP2 blots confirm that the bleach-induced bands that appear above the normal MAP2 position contain MAP2. The complexity of these bands, seen as smearing on the gel, is reduced when DTAF-tubulin is a smaller fraction of the total tubulin at the time of bleaching. The anti-β-tubulin blots show that both the 145,000-mol-wt band and some of the high-molecular-weight material on the gel contain tubulin. α-Tubulin does not appear to become cross-linked during bleaching, but the possibility of antigen masking or alteration during cross-linking makes this negative result of tenuous significance.

The disappearance of the MAP2 band as a result of irradiation suggests that the loss of polymerization competence with irradiation might be due to inactivation of the MAPs. This possibility has been excluded by bleaching tubulin before the addition of MAPs or after MAP addition but before warming to induce polymerization. DTAF-tubulin is rendered inactive by slow bleaching in PME-GTP at any of these times, but as expected, the MAP2 band is lost only if the MAPs are present during irradiation. The extent of their loss is less when the protein is bleached before polymerization (data not shown).

Tubulin without added MAPs was assembled in PME-GTP supplemented with taxol (10 μM) and bleached over 5 min with the expanded laser beam. A significant disassembly of DTAF-MTs accompanied the bleach, as determined by OD_{350}, but the control MTs were unaffected. DTAF-tubulin was not assembly competent in taxol after the bleach. The 145,000-mol-wt band appeared after the bleach in taxol, but the band running just above MAP2 did not. The diffuse bands visible at the top of the gel were much less dense than the bands observed in similar experiments with MAPs present (data not shown). DTAF-tubulin (2.0 mg/ml) which had been inactivated by bleaching could not be driven to polymerize by the addition of 10 mM taxol to a final concentration of 20 μM.

Addition of 4 mM ascorbate, a scavenger of free radicals (6), protects DTAF-tubulin in PME-GTP against the effects of laser irradiation. After a 5-min treatment with the spread beam, DTAF-tubulin in ascorbate is still assembly competent, the MAPs bands are not lost from the gels, and there is little decrease in OD_{490}. If the ascorbate-assembly mixture is irra-

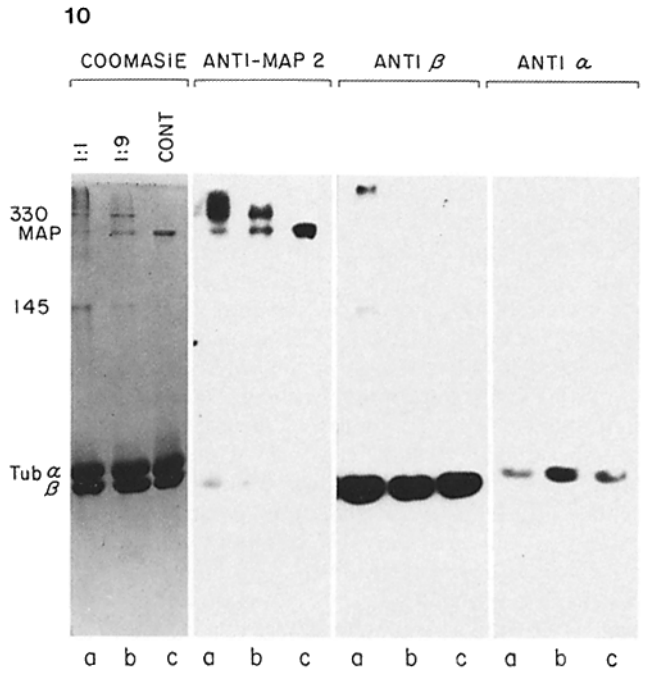

FIGURE 10 Antibody staining of bleached DTAF-tubulin. Microtubules were assembled from a mixture of equal parts DTAF-tubulin and control tubulin (*a*), a mixture of one part DTAF-tubulin to nine parts control tubulin (*b*), and control tubulin alone (*c*). These mixtures were bleached with the spread laser beam to 80% of their original fluorescence and electrophoresed on a 4–11% acrylamide SDS gel. The protein bands were electrophoretically transferred to nitrocellulose paper and stained with mouse monoclonal antibodies to α-tubulin, β-tubulin, and MAP2. The nitrocellulose sheets were secondarily stained with ^{125}I-goat anti-mouse IgG and autoradiograms were prepared. Anti-α-tubulin stains only the α-tubulin bands. Anti-MAP2 stains the MAP2 bands and high-molecular-weight aggregates (mol wt > MAP2) that form after bleaching. The specificity of aggregation increases as the DTAF-tubulin is diluted. Anti-β-tubulin stains β-tubulin, the 145,000-mol wt band, and a-band at the top of the gel which is also labeled by anti-MAP2. One band appears to be an aggregate of MAP2 and β-tubulin. The reasons for the shift in mobility of other MAP2 bands remains obscure. These staining patterns are difficult to interpret because covalent aggregation might restrict access to antigenic sites.

diated until a decrease in OD_{490} is observed (about five times the exposure necessary in the absence of ascorbate), the loss of the MAPs bands occurs, and there is an equivalent loss of assembly competence (data not shown).

Effects of fast bleaches (0.5 s) on the fine structure of MTs were studied. MTs assembled from a 1:9 mixture of DTAF-tubulin and cycle 2 MT protein were adsorbed to a Formvar-coated finder grid. An area within a grid square was exposed to a 0.5-s irradiation from the laser microbeam and then the grid was moved and irradiated again until the entire grid square had been exposed to the microbeam. The grid was then processed for electron microscopy by negative staining with uranyl acetate. We compared electron microscopic images of MTs in the area that had been bleached with MTs in areas that had not been bleached. No differences were observed.

MT Length Distribution

Turbidity of solutions containing MTs gives information about the quantity of polymer but not the lengths of individual MTs. We used the electron microscope to test the possibility that DTAF-MTs might be fragmented by laser irradiation. The mean lengths for control MTs and DTAF-MTs slow-bleached in PME-GTP were determined to be 3.0 μm ± 2.2 μm (n = 100) and 2.8 μm ± 1.7 (n = 100), respectively. These values were not signficantly different at a 95% confidence level.

Conditions That Minimize Bleach-induced Artifact In Vitro

Fig. 11 compares the effects of bleaches performed in PME-GTP over 5 min with those performed in PME-GTP supplemented with 2 mM glutathione over 5 min and with bleaches in the latter buffer achieved in 0.5 s with the capillary flow

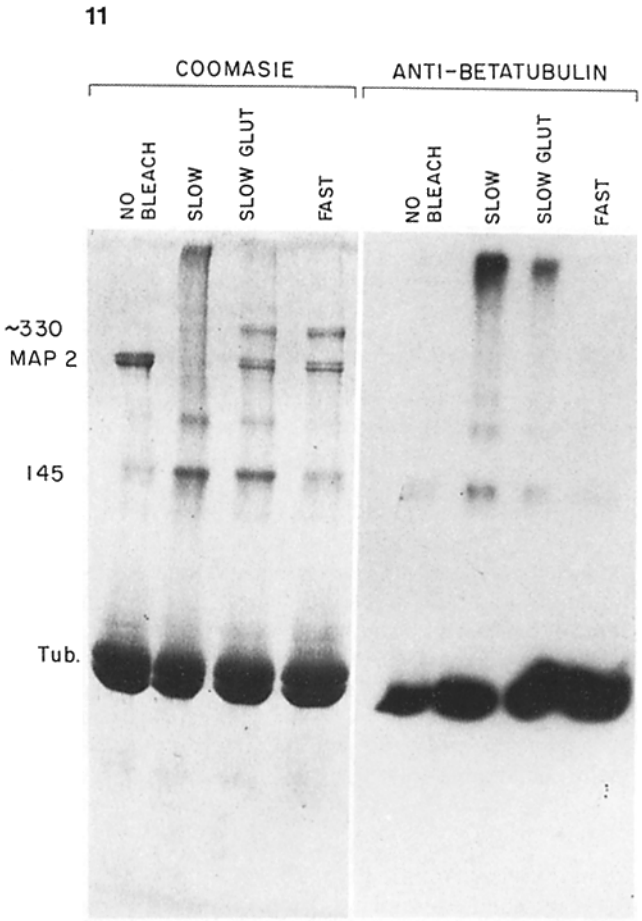

FIGURE 11 Comparison of the effects of slow and fast bleaching, with and without glutathione. DTAF-MTs were bleached slowly (5 min) in quartz cuvettes and fast (1 s) in capillaries. Aliquots taken before bleaching, after slow bleaching, after slow bleaching in glutathione (SLOW GLUT), and after fast bleaching were electrophoresed on a 4–11% polyacrylamide SDS gel and stained with Coomassie Blue. Identical lanes were transferred electrophoretically to nitrocellulose paper and stained with a mouse monoclonal anti-β-tubulin, then secondarily stained with ^{125}I-goat anti-mouse IgG. The control shows the MAP2 bands, a small amount of 145,000-mol wt aggregate and two tubulin bands. A slow bleach reduces the density of the MAP2 bands, intensifies the 145,000-mol wt band, and creates a smear of protein at the top of the gel. Aggregation is greatly reduced when DTAF-MTs are bleached in the presence of 2 mM reduced glutathione (SLOW GLUT). Fast bleaches (FAST) also reduce the extent of aggregation, particularly that involving β-tubulin.

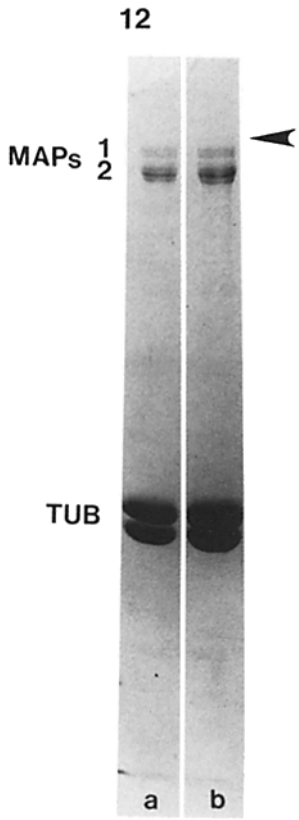

FIGURE 12 SDS gel electrophoresis of diluted, fast-bleached DTAF-tubulin in glutathione. A mixture of twice-cycled bovine brain MT protein (2.25 mg/ml) and DTAF-tubulin (0.2 mg/ml) was assembled in PME-GTP and 2 mM glutathione, then bleached in a capillary for 0.5 s. 10-μg samples of this protein were electrophoresed on a 4–11% polyacrylamide gradient gel in the presence of SDS. Bands corresponding to tubulin (*TUB*) and MAPs *1* and *2* are present in lane *a* before bleaching. After the bleach the protein bands in lane *b* are similar to those observed in lane *a*. The arrowhead points to a faint band in lane *b* that is not present in lane *a*.

cell. Coomassie staining is displayed beside an immume blot using anti-β-tubulin. The results show that glutathione inhibits the formation of irradiation-induced covalent links between proteins. Fast bleaching also reduces the extent of protein cross-linking. Fig. 12 shows an SDS gel analysis of DTAF-tubulin before and after bleaching, combining all of the factors so far identified to reduce irradiation damage to protein behavior: dilution with control protein, addition of glutathione (both of which occur during protein microinjection into a living cell), and fast bleaching with intense light (as occurs in cellular microbeam studies). Comparison of lanes *a* and *b* shows almost no change with bleaching. These results are consistent with Fig. 8*b*, which shows that the same experimental conditions preserve assembly competence.

DISCUSSION

We have characterized tubulin labeled with DTAF, by using assays and conditions in vitro that parallel the experiments in vivo described in the subsequent articles of this series. In agreement with published work (21, 51), we have found that the kinetic characteristics and assembled structures of unbleached DTAF-tubulin are indistinguishable from those of unlabeled control tubulin. DTAF-tubulin also elongates axonemes in a biased polar fashion, as demonstrated for unlabeled tubulin by Snell et al. (45), Allen and Borisy (1), and many others. Like unlabeled tubulin, it adds to the distal ends of MTs initiated by a centrosome in vitro (12). When bleached in PME-GTP with brain MAPs present, DTAF-MTs stay polymerized, but after depolymerization the subunits behave differently from irradiated control protein. Under some conditions of irradiation, covalent links form between DTAF-tubulin and other proteins and MT subunits lose assembly activity. Even some of the uncross-linked protein loses assembly activity. When DTAF-tubulin is bleached rapidly in the presence of physiological concentrations of glutathione and in concentrations of unlabeled protein comparable with those used for studies of fluorescence redistribution after photobleaching in vivo, we detect no deleterious effects of laser photobleaching on the behavior of the protein in vitro.

The protein aggregates that form during bleaching in PME-GTP have not been fully characterized, but we have some clues to their nature. The correlation between bleaching of DTAF in PME-GTP and the protein cross-linking events is clear: aggregates do not form when control assembly mixtures are irradiated. MAPs bands are lost from the electrophoresis gels only when the MAPs are present during irradiation. In the presence of 4 mM L-ascorbate, a free-radical scavenger (6), DTAF is protected from bleaching, and aggregates do not form unless the irradiation time is increased to yield a comparable reduction in the OD_{490} of DTAF-tubulin. Apparently both bleaching and cross-linking depend on free-radical reactions. The efficacy of glutathione, which is a sulfhydryl reagent as well as a scavenger of free radicals, in blocking protein cross-linking and protecting tubulin against loss of polymerization activity suggests that sulfhydryl groups on the proteins are important in the damage done to DTAF-tubulin through laser bleaching.

Specific antibody staining demonstrates that the 145,000-mol-wt band and the diffuse high-molecular-weight bands observed with SDS PAGE both contain tubulin. The 145,000-mol-wt band might be a tubulin trimer or a cross-linked dimer that behaves anomalously on SDS gels. The appearance of a faint additional, tubulin-containing band with M_r = 205,000 (a potential tetramer) during slow bleaching in PME-GTP is further evidence for tubulin cross-linking during irradiation (Fig. 11). Indeed, the bands that appear above MAP2 run more slowly than MAP2 by increments corresponding to ~55 M_r, the mass of a tubulin subunit (Fig. 9–11), but reliable molecular weight standards in this region of the gel were not available.

Not all the cross-linking data are compatible with the hypothesis that DTAF is itself a photoactivatable cross-linker. The fact that immune blots show β-tubulin bound only to the aggregates of very high molecular weight, whereas well-defined aggregates that run just slower than MAP2 fail to bind β-tubulin antibody suggests that other cross-links may be forming. Sheetz and Koppel observed that the bleaching of fluorescein-concanavalin A bound to the outside of a red blood cell could induce cross-linking of spectrin on the inner surface of the membrane (43). Apparently the chemistry that accompanies bleaching can act at a distance from the site of bleaching, and the aggregates we see may include MAP–MAP bonds as well as tubulin–tubulin and tubulin–MAP bonds. Certainly the inactivation of all the DTAF-tubulin by slow bleaching in PME-GTP when only a fraction of the protein becomes bleached or cross-linked shows that the results of irradiation are complex. The general loss of tubulin polymerization activity with slow bleaching may be a factor in the loss of OD_{350} we have observed in many slow-bleach experiments. Inactivation of the bulk of the soluble tubulin may result in some MT disassembly over the 5 min of the slow bleach.

The specificity of the bleach-dependent cross-linking seen on SDS PAGE seems to improve when the DTAF-tubulin is in low concentration relative to control tubulin. When undiluted DTAF-tubulin is bleached, the diffuse bands at the top of the gel predominate over the "330,000-mol-wt" band, while the opposite is true when DTAF-tubulin is diluted 1:9. This phenomenon is most likely caused by the increased probabil-

ity that a MAP will be cross-linked to several tubulin monomers when DTAF-tubulin is undiluted.

The observation that β-tubulin becomes cross-linked to MAP2 during bleaching in PME-GTP suggests that these two molecules are near neighbors in MTs. The lack of cross-linking with α-tubulin carries little meaning, however, both because α-tubulin is usually less labeled than β and because the lack of link formation may derive from the chemical details of the protein–protein interaction rather than from a lack of contact.

Two subtleties of the experiments described in Figs. 4 and 5 are particularly important for interpreting experiments with fluorescent tubulin in vivo. The distributions of fluorescence seen in Figs. 4*b* and 5*c* show that DTAF-tubulin does not bind strongly to the lateral surfaces of existing MTs. Although there is faint staining of the preexisting polymer, it is negligible compared with the fluorescence seen at the MT ends where polymer elongation is occurring. DTAF-tubulin therefore appears to be incorporating into a MT surface lattice, rather than binding adventitiously to an existing MT wall. Fig. 5, *d–f* show that bleaching of DTAF-MTs in vitro does not change this situation. Indeed, the incorporation of DTAF-tubulin into the walls of MTs made of bleached DTAF-tubulin was so slow in vitro as to be unmeasurable (<5% fluorescence recovery in 1 h, data not shown). Fluorescence added largely at the MT ends. This observation confirms the results from polymer length distributions measured by electron microscopy that bleaching does not break MTs. It also suggests that bleaching of DTAF-MTs in vitro does not induce submicroscopic lesions that induce a rapid repair process by exchange of soluble subunits for those in the irradiated polymers. Our observations, combined with those of Keith et al. (21) and Wadsworth and Sloboda (51), encourage the view that DTAF-tubulin is a good probe for tubulin behavior in vivo, the subject of the following three articles in this series.

We are grateful to Mark Kirschner for his collaboration in developing the active centrosome preparations used here.

The work in Boulder was supported by grants from the National Institutes of Health (GM-31213), the National Science Foundation (PMC-80-14549), and the American Cancer Society (CD8) to Dr. McIntosh. The taxol was a gift from the Natural Products Branch of the National Cancer Institute.

Address requests for reprints to Dr. McIntosh.

Received for publication 26 March 1984, and in revised form 13 August 1984.

REFERENCES

1. Allen, C., and G. G. Borisy. 1974. Structural polarity and directional growth of microtubules of *Chlamydomonas* flagella. *J. Mol. Biol.* 90:381–402.
2. Batteiger, B., W. J. Newhall, and R. B. Jones. 1982. The use of Tween 20 as a blocking agent in the immunological detection of proteins transferred to nitrocellulose membranes. *J. Immunol. Methods.* 55:297–307.
3. Bergen, L. G., and G. G. Borisy. 1980. Head to tail polymerization of microtubules in vitro. Electron microscope analysis of seeded assembly. *J. Cell Biol.* 84:141–150.
4. Bradford, M. M. 1976. A rapid and sensitive method for the quantitation of microgram quantities of protein utilizing the principle of protein-dye binding. *Anal. Biochem.* 72:248–254.
5. Bryan, J. 1976. A quantitative analysis of microtubule elongation. *J. Cell Biol.* 71:749–767.
6. Cooper, J. B., and J. E. Varner. 1983. Insolubilization of hydroxyproline-rich cell wall glycoprotein in aerated carrot root slices. *Biochem. Biophys. Res. Commun.* 112:161–167.
7. Erickson, P. F., L. N. Minier, and R. S. Lasher. 1982. Quantitative electrophoretic transfers of polypeptides from SDS polyacrylamide gels to nitrocellulose sheets: a method for their re-use in immunoautoradiographic detection of antigens. *J. Immunol. Methods.* 51:241–249.
8. Freud, J. E. 1971. Mathematical Statistics. Prentice-Hall, Engelwood Cliffs, NJ. 2nd edition. 463 pp.
9. Gibbons, I. R. 1965. Chemical dissection of cilia. *Arch. Biol.* 76:317–352.
10. Giloh, H., and J. W. Sedat. 1982. Fluorescence microscopy: reduced photobleaching of rhodamine and fluorescein protein conjugates by *n*-propyl gallate. *Science (Wash. DC).* 217:1252–1255.
11. Hamel, E., and C. M. Lin. 1981. Glutamate-induced polymerization of tubulin: characteristics of the reaction and application to large-scale purification of tubulin. *Arch. Biochem. Biophys.* 209:29–40.
12. Heidemann, S. R., G. W. Zieve, and J. R. McIntosh. 1980. Evidence for microtubule subunit addition to the distal end of mitotic structures in vitro. *J. Cell Biol.* 87:152–159.
13. Inoue, S. 1952. The effect of colchicine on the microscopic and submicroscopic structure of the mitotic spindle. *Exp. Cell Res.* Supplement 2:305–318.
14. Inoue, S. 1952. Effect of temperature on the birefringence of the mitotic spindle. *Biol. Bull. (Woods Hole).* 103:316.
15. Inoue, S., and H. Sato. 1967. Cell motility by labile association of molecules: the nature of mitotic spindle fibers and their role in chromosome movement. *J. Gen. Physiol.* 50:259–292.
16. Izant, J. G. 1983. The role of calcium ions during mitosis. *Chromosoma (Berl.).* 88:1–10.
17. Izant, J. G., and J. R. McIntosh. 1980. Microtubule-associated proteins: a monoclonal antibody to MAP2 binds to differentiated neurons. *Proc. Natl. Acad. Sci. USA.* 77:4741–4745.
18. Izant, J. G., J. A. Weatherbee, and J. R. McIntosh. 1983. A microtubule-associated protein antigen unique to mitotic spindle microtubules in PtK_1 cells. *J. Cell Biol.* 96:424–434.
19. Jacobson, K., Z. Dersko, E.-S. Yu, Y. Hou, and G. Poste. 1976. Measurement of the lateral motility of cell surface components by fluorescence recovery after photobleaching. *J. Supramol. Struct.* 5:565–576.
20. Jacobson, K., E. Elson, D. Koppel, and W. Webb. 1983. International workshop on the application of fluorescence photobleaching techniques to problems in cell biology. *Fed. Proc.* 42:72–79.
21. Keith, C. H., J. R. Feramisco, and M. Shelanski. 1981. Direct visualization of fluorescein-labeled microtubules in vitro and in microinjected fibroblasts. *J. Cell Biol.* 88:234–240.
22. Keihart, D. P. 1981. Studies on the *in vivo* sensitivity of spindle microtubules to calcium ions and evidence for a vesicular calcium-sequestering system. *J. Cell Biol.* 88:604–617.
23. Kilmartin, J. V., B. Wright, and C. Milsten. 1982. Rat monoclonal anti-tubulin antibodies derived by using a new nonsecreting rat cell line. *J. Cell Biol.* 93:576–582.
24. Kim, H., L. I. Binder, and J. L. Rosenbaum. 1979. The periodic association of MAP2 with brain microtubules in vitro. *J. Cell Biol.* 80:266–276.
25. Kosower, N. S., and E. M. Kosower. 1978. The glutathione status of cells. *Int. Rev. Cytol.* 55:109–160.
26. Kreis, T. E., and W. Birchmeier. 1982. Microinjection of fluorescently labeled proteins into living cells with emphasis on cytoskeletal proteins. *Int. Rev. Cytol.* 75:209–228.
27. Kreis, T. E., B. Geiger, and J. Schlessinger. 1982. Mobility of microinjected rhodamine actin within living chicken gizzard cells determined by fluorescence photobleaching recovery. *Cell.* 29:835–845.
28. Laemmli, U. K. 1971. Cleavage of structural proteins during the assembly of the head of bacteriophage T4. *Nature (Lond.).* 227:680–685.
29. Lanni, F., D. L. Taylor, and B. R. Ware. 1981. Fluorescence photobleaching recovery in solutions of labeled actin. *Biophys. J.* 35:351–364.
30. Margolis, R. L., and L. Wilson. 1978. Opposite end assembly and disassembly of microtubules at steady state *in vitro*. *Cell.* 13:1–8.
31. McIntosh, J. R. 1983. The centrosome as an organizer of the cytoskeleton. *In* Spatial Organization of Eukaryotic Cells. J. R. McIntosh, editor. A. R. Liss, New York. 115–142.
32. Meister, A., and S. S. Tate. 1976. Glutathione and related gamma-glutamyl compounds: biosynthesis and utilization. *Annu. Rev. Biochem.* 45:559–604.
33. Mitchison, T. J., and M. W. Kirschner. 1983. Purification and properties of mammalian microtubule organizing centers. *J. Cell Biol.* 97:254a. (Abstr.)
34. Murphy, D. B., and G. G. Borisy. 1975. Association of high-molecular-weight proteins with microtubules and their role in microtubule assembly *in vitro*. *Proc. Natl. Acad. Sci. USA.* 72:2696–2700.
35. O'Farrell, P. H. 1975. High resolution two-dimensional electrophoresis of proteins. *J. Biol. Chem.* 250:4007–4021.
36. Rebhun, L. I., M. Miller, T. C. Schnaitman, J. Nath, and M. Mollon. 1976. Cyclic nucleotides, thiodisulfide status of proteins, and cellular control processes. *J. Supramol. Struct.* 5:199–219.
37. Salmon, E. D. 1975. Pressure-induced depolymerization of spindle microtubules. *J. Cell Biol.* 65:603–614.
38. Salmon, E. D., R. J. Leslie, W. M. Saxton, M. Karow, and J. R. McIntosh. 1984. Spindle microtubule dynamics in sea urchin embryos. Analysis using fluorescence-labeled tubulin and measurements of fluorescence redistribution after laser photobleaching. *J. Cell Biol.* 99:2165–2174.
39. Salmon, E. D., M. Saxton, R. J. Leslie, M. L. Karow, and J. R. McIntosh. 1984. Diffusion coefficient of fluorescein-labeled tubulin in the cytoplasm of embryonic cells of the sea urchin *Lytechinus variegatus*. *J. Cell Biol.* 99:2157–2164.
40. Saxon, W. M., D. L. Stemple, R. J. Leslie, E. D. Salmon, and J. R. McIntosh. 1984. Tubulin dynamics in cultured mammalian cells. *J. Cell Biol.* 99:2175–2186.
41. Schmidt, W. J. 1939. Doppelbrechung der kerspindel und zugfasertheorie der chromosomenbewegung. *Chromosomal (Berl.).* 1:253–264.
42. Scholey, J. M., B. Neighbors, E. D. Salmon, and J. R. McIntosh. 1984. Isolation of microtubules and a dynein-like MgATPase from unfertilized sea urchin eggs. *J. Biol. Chem.* 259:6516–6525.
43. Sheetz, M. P., and D. E. Koppel. 1979. Membrane damage caused by irradiation of fluorescent concanavalin A. *Proc. Natl. Acad. Sci. USA.* 76:3314–3317.
44. Sloboda, R. D., W. L. Dentler, and J. L. Rosenbaum. 1976. Microtubule-associated proteins and the stimulation of tubulin assembly *in vitro*. *Biochemistry.* 15:4497–4505.
45. Snell, W. J., W. L. Dentler, L. T. Haimo, L. I. Binder, and J. L. Rosenbaum. 1974. Assembly of chick brain tubulin onto isolated basal bodies of *Chlamydomonas reinhardi*. *Science (Wash. DC).* 185:357–360.
46. Taylor, D. L., P. A. Amato, K. Luby-Phelps, and P. McNeil. 1984. Fluorescent analog cytochemistry. *Trends Biochem. Sci.* 9:88–91.
47. Taylor, D. L., and Y.-L. Wang. 1978. Molecular cytochemistry: incorporation of fluorescently labeled actin into living cells. *Proc. Natl. Acad. Sci. USA.* 75:857–861.
48. Towbin, H., T. Staehlin, and J. Gordon. 1979. Electrophoretic transfer of proteins from polyacrylamide gels to nitrocellulose sheets: procedure and some applications. *Proc. Natl. Acad. Sci. USA.* 76:4350–4354.
49. Travis, J. L., R. D. Allen, and R. D. Sloboda. 1980. Preparation and characterization of native, fluorescently labeled brain tubulin and microtubule associated proteins. *Exp.*

Cell Res. 125:421–429.
50. Wadsworth, P., and R. D. Sloboda. 1982. Characterization of tubulin modified with the sulfhydryl-reactive fluorochrome monobromo(trimethylamino)bimane. *Biochemistry.* 21:21–28.
51. Wadsworth, P., and R. D. Sloboda. 1983. Microinjection of fluorescent tubulin into dividing sea urchin cells. *J. Cell Biol.* 97:1249–1254.
52. Wang, K. J., R. Feramisco, J. F. Ash. 1983. Fluorescent localization of contractile proteins in tissue culture cells. *Methods Enzymol.* 85:514–562.
53. Wang, Y.-L., J. M. Heiple, and D. L. Taylor. 1982. Fluorescent analog cytochemistry of contractile proteins. *Methods Cell Biol.* 25:1–11.
54. Wang, Y.-L., F. Lanni, P. L. McNeil, B. R. Ware, and D. L. Taylor. 1982. Mobility of cytoplasmic and membrane-associated actin in living cells. *Proc. Natl. Acad. Sci. USA.* 79:4660–4664.
55. Webb, W. W., L. S. Barak, D. W. Tank, and E.-S. Wu. 1980. Molecular mobility on the cell surface. *Biochem. Soc. Symp.* 46:191–205.
56. Weingarten, M. D., A. H. Lockwood, S. Hwo, and M. W. Kirschner. 1975. A protein factor essential for microtubule assembly. *Proc. Natl. Acad. Sci. USA.* 72:1858–1862.
57. Weingarten, M. D., M. M. Suter, D. R. Littman, and M. W. Kirschner. 1974. Properties of the depolymerization products of microtubules from mammalian brain. *Biochemistry.* 13:5529–5537.
58. Weisenberg, R. C. 1972. Microtubule formation *in vitro* in solutions containing low calcium concentrations. *Science (Wash. DC).* 177:1104–1105.
59. Willingham, M. C., and I. Pastan. 1978. The visualization of fluorescent proteins in living cells by video intensification microscopy. *Cell.* 13:501–507.
60. Wilson, L., K. B. Snyder, W. C. Thompson, and R. L. Margolis. 1982. A rapid filtration assay for analysis of microtubule assembly, disassembly, and steady-state tubulin flux. *Methods Cell Biol.* 24:159–169.
61. Wojcieszyn, J. W., R. A. Schlegel, E. S. Wu, and K. Jacobson. 1981. Diffusion of injected macromolecules within the cytoplasm of living cells. *Proc. Natl. Acad. Sci. USA.* 78:4407–4410.